PACS 62.20.fq, 81.40.Ef, 81.40.Lm

Effect of Chemical Composition and Grain Size on RT Superplasticity of Zn-Al alloys processed by ECAP

M. Demirtas[1], G. Purcek[2†], H. Yanar[2], Z.J. Zhang[3], Z.F. Zhang[3]

[†]purcek@ktu.edu.tr

[1]Department of Mechanical Engineering, Bayburt University, Bayburt 69000, Turkey
[2]Department of Mechanical Engineering, Karadeniz Technical University, Trabzon 61080, Turkey
[3]Shenyang National Laboratory for Materials Science, Institute of Metal Research, Chinese Academy of Sciences, Shenyang 110016, China

Dilute Zn-0.3Al, eutectic Zn-5Al and eutectoid Zn-22Al alloys were processed by multi-pass equal channel angular pressing (ECAP) in order to achieve fine grained (FG) or ultrafine-grained (UFG) microstructure and room temperature (RT) superplasticity. ECAP refined the microstructure of Zn-0.3Al and resulted in a FG Zn-rich η-matrix with an average grain size of 2 μm and homogeneously distributed nano-sized Al-rich α-particles with the grain sizes in the range of 50-200 nm. A bi-modal microstructure was achieved in Zn-5Al alloy with UFG Al-rich α– and FG Zn-rich η–phases having mean grain sizes of 110 nm and 540 nm, respectively. ECAP brought about an agglomerate-free UFG microstructure in Zn-22Al alloy with an average grain size of 200 nm which is the lowest one obtained so far for this alloy after ECAP processing. The maximum RT superplastic elongations of 1000%, 520% and 400% were achieved for Zn-0.3Al, Zn-5Al and Zn-22Al alloys, respectively. Considering the RT superplasticity in Zn-Al alloys, it was found that lower Al content results in higher superplastic elongations even if the alloy has relatively larger grain size. Grain boundary sliding (GBS) was found to be the main deformation mechanism in region-II as the optimum superplastic region during RT deformation for all three Zn-Al alloys with the strain rate sensitivity factor ranging between 0.25-0.31.

Keywords: Zn-Al alloys, room temperature superplasticity, ultrafine-grained materials, equal channel angular pressing

Влияние химического состава и размера зерен на сверхпластичность при комнатной температуре сплавов Zn-Al, подвергнутых РКУП

Низколегированный сплав Zn-0.3Al, эвтектик Zn-5Al и эвтектоидный сплав Zn-22Al были подвергнуты многопроходному равноканальному угловому прессованию (РКУП) с целью получения мелкозернистой (МЗ) или ультрамелкозернистой (УМЗ) структуры и достижения сверхпластичности при комнатной температуре. РКУП привело к измельчению микроструктуры Zn-0.3Al и формированию МЗ обогащенной Zn η-матрицы со средним размером зерен 2 мкм и однородно распределенных наноразмерных богатых Al α-частиц с размером в интервале 50-200 нм. В сплаве Zn-5Al была получена бимодальная структура с УМЗ богатой Al α– фазой и МЗ богатой Zn η– фазой, имеющими соответственно размеры зерен 110 нм и 540 нм. В сплаве Zn-22Al РКУП привело к формированию не агломерированной УМЗ микроструктуры со средним размером зерен 200 нм, что представляет собой минимальное достигнутое к настоящему времени значение размера зерен, полученное РКУП на данном сплаве. Для сплавов Zn-0.3Al, Zn-5Al и Zn-22Al были получены максимальные сверхпластические удлинения при комнатной температуре, равные соответственно 1000%, 520% и 400%. По отношению к сверхпластичности сплавов Zn-Al показано, что более низкое содержание Al приводит к более высоким сверхпластическим удлинениям, даже если сплав имеет больший размер зерен. Показано, что зернограничное проскальзывание (ЗГП) является основным механизмом деформации в области II, являющейся оптимальной областью сверхпластической деформации при комнатной температуре для всех трех сплавов Zn-Al с показателем скоростной чувствительности в интервале 0.25-0.31.

Ключевые слова: сплавы Zn-Al, сверхпластичность при комнатной температуре, ультрамелкозернистые материалы, равноканальное угловое прессование

1. Introduction

Polycrystalline materials can show extremely large neck-free elongations prior to failure when some microstructural and experimental conditions are fulfilled, which is known as superplasticity [1]. As a microstructural requirement, superplastic materials need to have at least fine grained (FG) duplex- or quasi-single phase microstructures with the grain sizes less than ~10 μm [2]. Regarding the experimental conditions to achieve superplasticity, firstly, tensile test temperature should be high, normally at or above $0.5T_m$, where T_m is the absolute melting temperature of the material, since superplasticity is a diffusion-controlled process [2]. The second experimental requirement is that the tensile tests should be performed at low strain rates ranging between 1×10^{-5} and 1×10^{-3} s^{-1}. All these requirements should be fulfilled so that the grain boundary sliding (GBS) can occur easily as the main deformation mechanism in superplastic region [3]. After the first report in 1912 [4], superplasticity-related studies have been one of the main topics among the material scientists and mechanical engineers, and various classes of materials including alloys [5—18], ceramics [19—21] and amorphous materials [22,23] have been addressed for this purpose.

Related to the superplastic studies, recently it has been aimed to achieve low temperature and high strain rate superplasticity in order to enhance the applications of superplasticity and to reduce the cost of superplastic forming. Furthermore, recent studies have shown that superplastic behavior can be achieved even at room temperature (RT) and high strain rates near or above 10^{-2} s^{-1} if the grain size of the superplastic material is decreased down to micron or sub-micron levels. For substantial grain refinement, on the other hand, new techniques have been proposed, which made possible to produce ultrafine-grained (UFG) or nanostructured (NS) materials. However, it should be noted that it is not possible to achieve RT superplasticity in all UFG or NS materials. RT and HSR superplastic behavior can be achieved in some specific alloys like Sn-Bi [24], Pb-Tl [25], Pb-Sn [26], and Zn-Al [5—18] due to their relatively low melting points. Among them, Zn-Al alloy family is the most suitable one as considering its phase diagram shown in Fig. 1. According to this phase diagram, three main regions seem to be suitable for superplastic behavior considering the phase structure. The first one is the eutectoid composition having 22wt.% Al content which is well known superplastic Zn-Al alloy (Zn-22Al) with duplex phase structure. The second one is the eutectic composition having 5wt.% Al content (Zn-5Al). This alloy has also duplex phase structure as in the case of Zn-22Al alloy. The third one is the compositions having very low Al content up to 1.1%, which are known as dilute Zn-Al alloys. The dilute alloys have quasi-single phase structure which is also suitable for superplastic behavior.

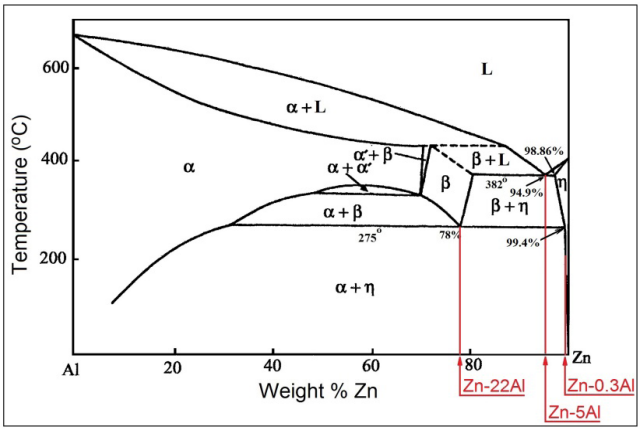

Fig. 1. Binary Zn-Al phase diagram [27].

2. Room temperature superplasticity of Zn-Al alloys

For achieving FG or UFG microstructure and obtain RT and HSR superplasticity in Zn-Al alloys some thermal and thermo-mechanical processes as well as severe plastic deformation (SPD) techniques like equal-channel angular pressing (ECAP) [11,13—18] and friction stir processing (FSP) [12] have been utilized. Previous studies on RT and HSR superplasticity in Zn-Al alloys and the main results achieved are listed in Table 1. From this table, aging was applied to Zn-22Al at 250°C for 30 min and refined its microstructure down

Table 1. RT tensile properties along with average grain size as a result of different processes obtained from previous reports on RT superplasticity of Zn-Al alloys (*df: grain size, T: tensile test temperature, ε̇: strain rate, ε_f elongation to failure*)

	Alloy	Process	d_f (μm)	T (°C)	$\dot{\varepsilon}$ (s^{-1})	Max. ε_f (%)	Ref.
Thermal processes	Zn-22Al	Aging	0.35	25	$1x10^{-3}$	125	[5]
Thermomechanical processes	Zn-0.2Al	Extrusion	1.6	25	$7x10^{-3}$	590	[6]
	Zn-0.3Al	Rolling	1	25	$2x10^{-4}$	1400	[7]
	Zn-0.4Al	Rolling	0.6	25	$6.67x10^{-4}$	>500	[8]
	Zn-1.1Al	Rolling	1	25	$1x10^{-3}$	~600	[9]
	Zn-22Al	Cryo-rolling	0.25	25	$4x10^{-3}$	335	[5]
		Extrusion	0.8	30	$1x10^{-5}$	340	[10]
SPD techniques	Zn-5Al	8 passes ECAP at RT	Bi-modal	25	$1x10^{-3}$	520	[11]
	Zn-22Al	FSP	0.6	25	$1x10^{-2}$	160	[12]
		4 passes ECAP at RT	0.35	25	$1x10^{-2}$	240	[13,14]
		8 passes ECAP at RT	0.55	25	$4x10^{-3}$	335	[5]
		4—24 passes ECAP at 200°C	0.7-0.9	25	$1x10^{-3}$	280	[15]
		8 passes ECAP at 200°C	1.3	25	$1x10^{-4}$	250	[16]
		8 passes ECAP 50°C	0.8	25	$1x10^{-2}$	250	[17]
		Two-step ECAP	0.2	25	$5x10^{-2}$	400	[18]

to 350 nm. This process resulted in a 125% RT elongation to failure at a strain rate of 1×10^{-3} s^{-1} [5].

Many reports have also been published on changes in the microstructure and RT superplastic behavior of Zn-Al alloys by application of conventional thermomechanical processes like rolling and extrusion [6—10]. Considering the dilute Zn-Al alloys, Zn-0.2Al, Zn-0.3Al, Zn-0.4Al and Zn-1.1Al alloys were studied for this purpose. Cook [6] processed Zn-0.2Al using extrusion performed at 30°C with an extrusion ratio of 42:1 and obtained 1.6 μm grain size. The alloy showed a maximum RT elongation of about 590% at a strain rate of 7×10^{-3} s^{-1} in that study. Ha *et al.* [7] studied RT superplasticity of Zn-0.3Al alloy and used a thermomechanical process including hot rolling at 220°C followed by heat treatment at 220°C for 30 min and final cold rolling at RT to refine its microstructure. This process resulted in an average grain size of around 1.0 μm and an elongation of 1400% at RT and 2×10^{-4} s^{-1} strain rate. Grain size of the Zn-0.4Al was reduced to 600 nm by application of RT rolling with a 90% reduction in thickness [8]. This FG microstructure brought about a maximum RT elongation of about 500% at 6.67×10^{-4} s^{-1} strain rate. Malek and *Lukáč* [9] rolled Zn-1.1Al at 300°C with a reduction of 45%, and further reduction of 90% was applied at RT. This process brought about 1.0 μm grain size and ~600% maximum elongation at 1×10^{-3} s^{-1} strain rate. Conventional plastic deformation techniques have also been used to refine the microstructure of Zn-22Al and achieve RT superplastic behavior. For this purpose Xia *et al.* [5] applied the cryo-rolling process to Zn-22Al alloy at –70°C and obtained 250 nm grain size with an aspect ratio of 2.6, and an elongation of 315% at 4×10^{-3} s^{-1}. In another study, Zn-22Al alloy was subjected to extrusion from 150 mm to 10 mm diameter [10]. This process resulted in an 800 nm grain size and 340% RT elongation at 1×10^{-5} s^{-1}.

Regarding the SPD techniques, there is no study aiming to achieve RT superplasticity in dilute Zn-Al alloys. Demirtas *et al.* [11] processed Zn-5Al alloy using ECAP and achieved RT superplasticity in this alloy for the first time. In that study, a bimodal microstructure having 540 nm grain size of Zn-rich grains and 110 nm grain size of Al-rich grains was obtained. This bimodal microstructure resulted in a 520% elongation at RT and 1×10^{-3} s^{-1} strain rate. Zn-22Al is the most studied one among Zn-Al alloys for achieving RT superplasticity by means of SPD techniques. FSP has been applied to Zn-22Al alloy and it was seen that this process has no considerable effect on RT superplasticity of this alloy [12]. While FSP resulted in some grain refinement, limited increase in the superplastic elongation was obtained (elongation increased from 100% to 150% at a strain rate of 1×10^{-2} s^{-1}) after this process [12]. As the most commonly used SPD technique for achieving RT superplasticity in Zn-22Al alloy, ECAP has been applied to this alloy for gaining suitable microstructure for the superplasticity. Tanaka *et al.* [13,14] processed this alloy using ECAP at RT or 100°C and refined the microstructure down to 350 nm and 600 nm, respectively. In that study, the maximum elongation was achieved to be 240% at a strain rate of 1×10^{-2} s^{-1} after 4 passes RT ECAP. In another study, Xia *et al.* [5] showed that 10 μm initial grain size was reduced to 550 nm after 8 passes ECAP applied to Zn-22Al at RT, and 335% elongation was achieved at RT and 4×10^{-3} s^{-1} strain rate. Kumar *et al.* [15] investigated the effect of ECAP pass numbers on the grain size and superplastic behavior of Zn-22Al alloy having 1.8 μm initial grain size. They reported that the grain size was reduced to 800 nm and 700 nm after 4 and 8 passes ECAP performed at 200°C, respectively. In that study, 280% maximum elongation was achieved at a strain rate of 1×10^{-2} s^{-1}. Huang and Langdon [16] also studied the effect of ECAP on the microstructure and RT superplasticity of Zn-22Al alloy, and they obtained 1.3 μm grain size and 250% elongation at 1×10^{-4} s^{-1} after 8 passes ECAP at 200°C. Yang *et al.* [17] refined the grain size of the Zn-22Al to 800 nm and increased RT elongation to 250% at 1×10^{-2} s^{-1} by means of 8 passes ECAP performed at 50°C. More recently, Demirtas *et al.* [18] used a two-step ECAP process in which Zn-22Al alloy was subjected to 4 passes ECAP at 350°C followed by 4 passes ECAP at RT. This process brought about more refined microstructure with an average grain size of about 200 nm and resulted in the maximum RT elongation of about 400% at a relatively high strain rate of 5×10^{-2} s^{-1}. Torsional straining (TS) [28] and cross channel angular extrusion (CCAE) [29] have also been applied to eutectoid Zn-22Al alloy as grain refinement tool and resulted in significant grain refinement in Zn-22Al (350 nm and 300 nm grain sizes were achieved, respectively), but their effects on RT superplasticity of the alloy have not been studied.

In view of the above information, it can be concluded that RT superplastic behaviors of Zn-Al alloys with different compositions have been investigated individually, and no comparison has been undertaken so far. Especially, there is no study aiming to study the effects of grain size and phase structure on RT superplasticity of Zn-Al alloys. Therefore, the main objective of this study is to analyze the effects of alloy composition, phase structure and grain sizes of Zn-Al based superplastic alloys on their RT superplasticity at different strain rates, and compare the same set of the results. For this purpose, three Zn-Al alloys, dilute Zn-0.3Al, eutectic Zn-5Al and eutectoid Zn-22Al, were processed by multi-pass ECAP in order to achieve FG or UFG microstructure and RT superplasticity.

3. Effects of grain size and chemical composition on RT superplasticiy of Zn-Al alloys processed by ECAP

Three main Zn-Al alloys which are potential for RT superplasticity were processed by multi-pass ECAP using a die with 90° cross-sectional angle. Zn-0.3Al alloy was processed by 6 passes ECAP applied to the alloy at RT using route A where the billets are not rotated in-between subsequent passes. ECAP was performed following a hot rolling process at 100°C with 35% reduction in thickness. Eutectic Zn-5Al alloy was processed by 8 passes ECAP at RT [11]. ECAP was applied to Zn-22Al alloy as a two-step process. In the first step, 4 passes ECAP was applied to the alloy at 350°C, and 4 more passes were performed at RT as the second step [18]. Route Bc was used during ECAP processing of both Zn-5Al and Zn-22Al alloys where the billets are rotated by 90° in the same direction around their longitudinal axes in-between passes.

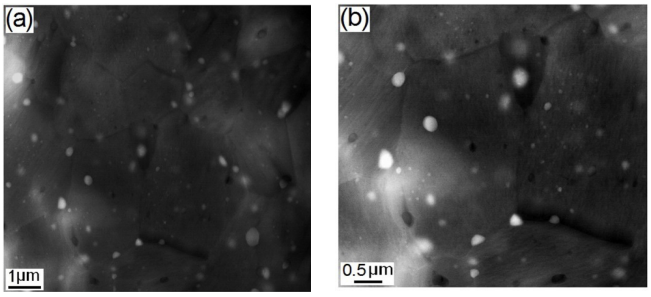

Fig. 2. (a) — (b) TEM micrographs showing the detailed microstructure of Zn-0.3Al alloy after ECAP.

TEM micrographs of the alloys after all processes are shown in Figs. 2–4. The processed microstructure of Zn-0.3Al alloy has FG Zn-rich η-matrix phase with an average grain size of about 2.0 μm and nano-sized Al-rich α-particles with the grain sizes in the range of 50—200 nm (Fig. 2a,b). The particles precipitated homogeneously throughout the microstructure both inside the grains and grain boundaries. Processing of Zn-5Al alloy brought about a bi-modal microstructure with UFG Al-rich α– and FG Zn-rich η — phases having mean grain sizes of 110 nm and 540 nm, respectively (Fig. 3a-c) [11]. Processing of Zn-22Al alloy resulted in an agglomerate-free UFG microstructure with an average grain size of 200 nm (Fig. 4a–c) [18]. In this microstructure, distributions of Al-rich α– and Zn-rich η – phases are quite homogeneous throughout the microstructure.

RT tensile test results at different strain rates (ranging from 1×10^{-4} to 1×10^{0} s^{-1}) are shown in Fig. 5 for all alloy compositions. Quasi-single phase Zn-0.3Al alloy showed the maximum RT elongation of around 1000% at a strain rate of 1×10^{-4} s^{-1} after ECAP (Fig. 5a), and elongation decreased with increasing strain rate. Elongations of 630%, 350%, 110% and 65% were obtained at the strain rates of 1×10^{-3} s^{-1}, 1×10^{-2} s^{-1}, 1×10^{-1} s^{-1} and 1×10^{0} s^{-1}, respectively, for this alloy. Compared to Zn-0.3Al alloy, duplex-phase Zn-5Al alloy showed lower superplastic elongations at low strain rates of 1×10^{-4} s^{-1} and 1×10^{-3} s^{-1}, but elongation values were measured to be slightly higher than that of Zn-0.3Al at higher strain rates. Maximum elongation was achieved to be 520% at 1×10^{-3} s^{-1} [11]. Below and above this strain rate, elongation to failure decreased, and 450%, 400%, 200% and 100% were obtained at 1×10^{-4} s^{-1}, 1×10^{-2} s^{-1}, 1×10^{-1} s^{-1} and 1×10^{0} s^{-1}, respectively (Fig.5b) [11]. Elongation to failure values of Zn-22Al alloy are smaller than that of both Zn-0.3Al and Zn-5Al alloys at and below 1×10^{-2} s^{-1} strain rate (Fig. 5c). However, Zn-22Al alloy showed higher superplastic elongation compared to two other alloys at high strain rates. Maximum elongation was achieved to be 400% at a high strain rate of 5×10^{-2} s^{-1} in this alloy [18]. Elongations of 245%, 185%, and 250% were achieved at the strain rates of 1×10^{-4} s^{-1}, 1×10^{-3} s^{-1} and 1×10^{-2} s^{-1}, respectively [18]. At high strain rates of 1×10^{-1} s^{-1} and 1×10^{0} s^{-1}, still high elongations of about 340% and 150% were obtained, respectively, in UFG Zn-22Al alloy (Fig. 5c) [18].

Changes in flow stresses with the initial strain rates for ECAPed Zn-0.3Al, Zn-5Al and Zn-22Al alloys are shown in Figs.5d—f, and strain rate sensitivity parameter, *m,* for the optimum superplastic regions were calculated from the slope of the stress-strain rate curves in these figures. Flow stresses of the alloys seem to be very sensitive to the initial strain rates, and increase with increasing strain rates. Region-II as the optimum superplastic region located between 1×10^{-4} and 1×10^{-3} s^{-1} strain rates for Zn-0.3Al having the *m*-value of around 0.31. On the other hand, Region-II for Zn-5Al alloy located between 1×10^{-4} and 1×10^{-2} s^{-1} strain rates with an *m*-

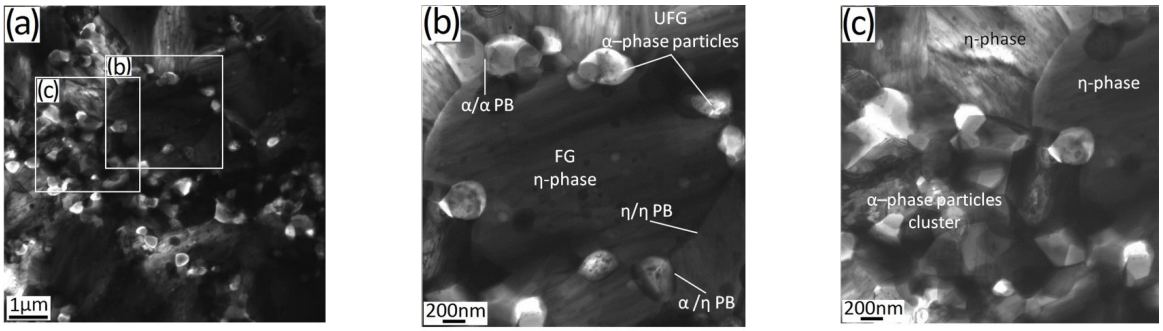

Fig. 3. (a) — (c) TEM micrographs showing the microstructure of Zn-5Al alloy after ECAP [11].

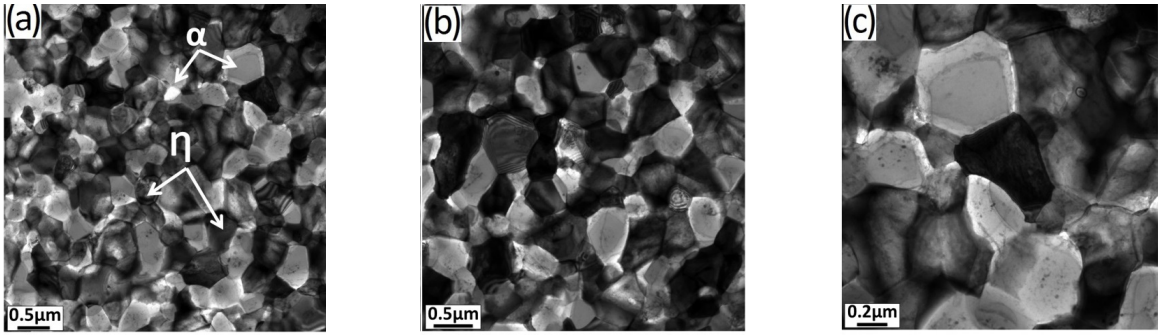

Fig. 4. (a) — (c) TEM micrographs showing the microstructure of Zn-22Al alloy after ECAP [18].

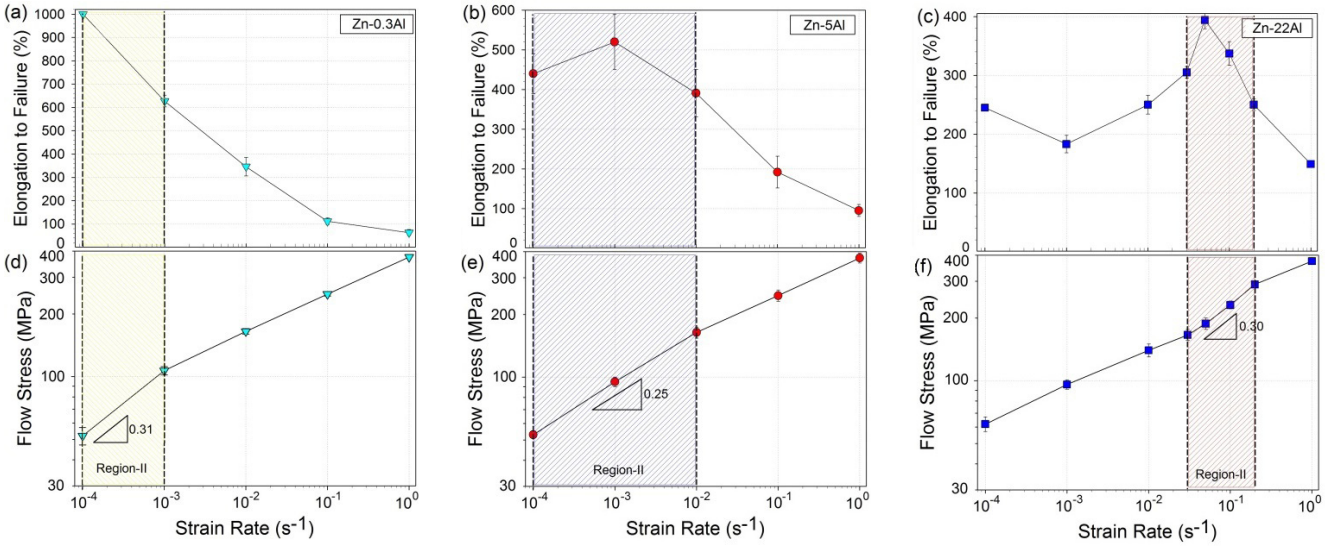

Fig. 5. (a) — (c) Changes in elongation to failure with initial strain rates, and (d) — (f) variation in flow stresses and m-values with initial strain rates.

value of 0.25. UFG microstructure formation in Zn-22Al alloy shifted Region-II to relatively higher strain rates between 3×10^{-2} s^{-1} and 2×10^{-1} s^{-1}. In this region, the *m*-value was 0.30.

It is known that decreasing grain size shifts the optimum superplastic region (region-II) to higher strain rates [30]. The results obtained for different Zn-Al alloys in the current study are consistent with that conclusion. Maximum elongation in Zn-22Al alloy having the smallest grain size occurred at a high strain rate of 5×10^{-2} s^{-1}. On the other hand, dilute Zn-0.3Al alloy with the highest grain size of 2 μm showed the maximum elongation at the lowest strain rate of 1×10^{-4} s^{-1}. Another effect of grain size on the superplastic materials is that decreasing grain size increases the superplastic elongation. However, considering the elongation to failure values obtained for different Zn-Al alloys having different microstructural features and compositions in the current study, the results are not consistent with that conclusion. The maximum elongation was achieved to be around 1000% in dilute Zn-0.3Al alloy with the highest grain size (2 μm) of Zn-rich matrix phase. On the other hand, Zn-22Al showed the lowest superplastic elongation although it has the smallest grain size of 200 nm. Regarding these results, it can be seen that phase composition has also a considerable effect on superplastic elongations of Zn-Al alloys. It is known that increasing content of the second phase also increases the microstructural stability of superplastic materials during the superplastic deformation at high temperature regime [3]. For this reason, eutectoid Zn-22Al alloy is the most favorable one for superplastic elongations especially at high temperatures among two other alloys. However, considering the superplastic deformation at RT chemical composition of the phase boundaries becomes more important than microstructural stability in Zn-Al alloys due to the low deformation temperature. It is known that GBS as the dominant deformation mechanism occurs mainly at the η/η and η/α phase boundaries and the α/α phase (or grain) boundaries do not slide easily in the Zn-Al alloys [31—34]. Decreasing the Al content in the Zn-Al alloys decreases the possibility of α/α phase boundary formation. This can be clearly seen in the TEM micrographs given in Figs. 2—4. In Zn-0.3Al alloy, almost all grain boundaries are in the form of η/η phase boundary (Fig. 2). Regarding eutectic Zn-5Al alloy, grain boundaries are either η/η or α/η and α/α phase boundaries are limited in the microstructure (Fig. 3). While some α/α boundaries are still exist in the microstructure of Zn-22Al alloy, homogeneous distribution of the α- and η-phases minimizes these boundaries (Fig. 4). From this conclusion, it is seen that increasing η/η phase boundaries also increases the possibility of grain boundary sliding which resulted in relatively high superplastic elongation. Thus, considering RT superplasticity in Zn-Al alloys, lower Al content results in higher superplastic elongations even if the alloy has relatively larger grain size.

4. RT superplastic deformation mechanisms of Zn-Al alloys processed by ECAP

It has been well established that GBS is the dominant deformation mechanism in superplasticity, and in the presence of GBS an *m*-value of 0.4 or higher is obtained in superplastic materials at elevated temperatures [35,36]. In the present study, ECAP-processed Zn-Al alloys have relatively lower strain rate sensitivity values ranging between 0.25 for Zn-5Al alloy and 0.31 for Zn-0.3Al. To determine the main deformation mechanisms in the optimum superplastic regions of the Zn-Al alloys, Zn-0.3Al, Zn-5Al and Zn-22Al were strained at 1×10^{-4} s^{-1} up to 65%, at 1×10^{-3} s^{-1} up to 100% and at 5×10^{-2} s^{-1} up to 100% and 130%, respectively. Each strain rate was chosen to be in the optimum superplastic region of the corresponding alloy. SEM micrographs showing the surface appearances of the samples after the deformation are shown in Figs. 6—8. From these micrographs, the evidence of GBS can be clearly seen. For all three alloys, most of the grain boundaries were revealed after straining as in the case of true superplasticity. In addition, the grains did not elongate along the tensile test direction (TTD) and they are still in the equiaxed grainy morphol-

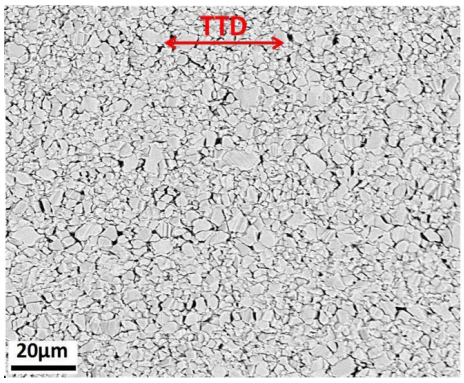

Fig. 6. SEM micrographs showing the surface appearance of Zn-0.3Al sample strained up to 65% at 1×10^{-4} s^{-1}.

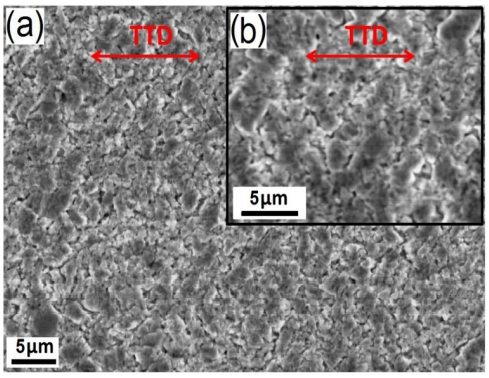

Fig. 7. SEM micrographs showing the surface appearance of Zn-5Al sample strained up to 100% at 1×10^{-3} s^{-1} [11].

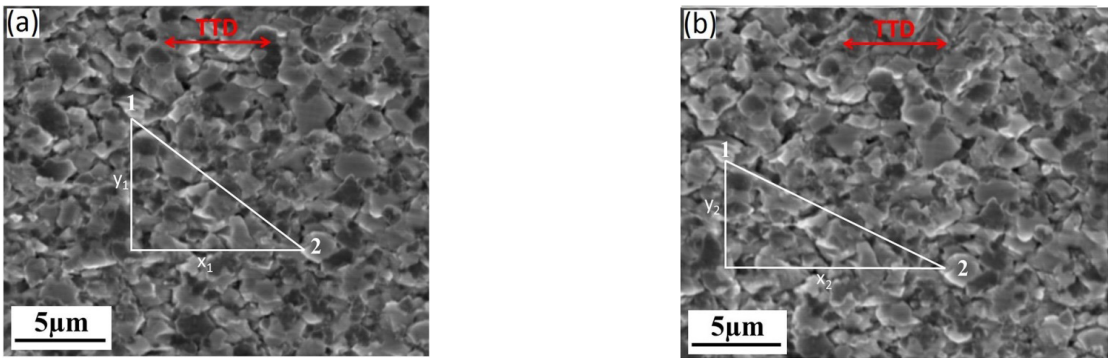

Fig. 8. SEM micrographs showing the surface appearance of Zn-22Al sample strained at 5×10^{-2} s^{-1} up to: (a) 100% and (b) 130% [18].

ogy even after straining. It is well known that the grains elongate along the TTD during the uniaxial straining in the absence of GBS in non-superplastic regions (region-I and region-III) [37]. In these regions, tensile test samples also elongate in this manner. Thus, the aforementioned observations suggest that GBS is the dominant deformation mechanism in the optimum superplastic regions of all three Zn-Al alloys. Another evidence of the occurrence of GBS in Zn-22Al alloy can be given as the change in vertical and horizontal distances between the grains numbered as «1» and «2» in Fig.8. It is clearly seen that 130% straining resulted in a decrease in the vertical distance between these grains ($y_1>y_2$) and brought about an increase in the horizontal distance along the TTD ($x_2>x_1$) as compared to those after 100% elongation. Since the equiaxed morphology of the grains did not change during deformation process, these grains separated each other due to the occurrence of the GBS [18]. It can be concluded that GBS is the dominant deformation mechanism in the optimum superplastic regions of all three Zn-Al alloys at RT despite the fact that the alloys have relatively lower strain rate sensitivity than that typical for occurrence of GBS during the superplastic deformation at high temperature regime.

5. Summary and conclusions

In this study, three Zn-Al alloys; dilute Zn-0.3Al, eutectic Zn-5Al and eutectoid Zn-22Al, were processed by multi-pass ECAP in order to achieve FG or UFG microstructure and RT superplasticity. The main results and conclusions of this study can be summarized as follows:

1. The ECAP processed microstructure of Zn-0.3Al alloy has FG Zn-rich η-matrix phases with an average grain size of about 2.0 μm and homogeneously distributed nano-sized Al-rich α-particles with the grain sizes in the range of 50—200 nm. ECAP resulted in a bi-modal microstructure with UFG Al-rich α– and FG Zn-rich η-phases having mean grain sizes of 110 nm and 540 nm, respectively, in Zn-5Al alloy. Processing of Zn-22Al alloy brought about an agglomerate-free UFG microstructure with an average grain size of 200 nm.

2. The maximum RT superplastic elongations of Zn-0.3Al, Zn-5Al and Zn-22Al alloys were measured to be 1000% at 1×10^{-4} s^{-1}, 520% at 1×10^{-3} s^{-1} and 400% at 5×10^{-2} s^{-1}, respectively.

3. It was confirmed that phase composition has also considerable effect on RT superplastic elongations of Zn-Al alloys beside the grain size. Considering the RT superplasticity in Zn-Al alloys, lower Al content results higher superplastic elongations even if the alloy has relatively larger grain size.

4. The effect of the phase composition on RT superplasticity of Zn-Al alloys is attributed to the differences between the grain boundary sliding (GBS) characteristics of different phase boundaries in these alloys. Since GBS as the dominant deformation mechanism occurs mainly at the η/η and η/α phase boundaries and the α/α phase (or grain) boundaries do not slide easily, decreasing Al content also decreases the possibility of α/α phase boundary formation and increases the superplastic elongation.

5. GBS was found to be the main deformation mechanism in region-II as the optimum superplastic region during the RT deformation in Zn-Al alloys having strain rate sensitivity ranging between 0.25—0.31.

Acknowledgements. This research was supported by Scientific Research Projects of Karadeniz Technical University, Turkey, under Grant no: 10501.

References

1. M. Kawasaki, T. G. Langdon, J. Mater. Sci. **49**, 6487 (2014).
2. T. G. Langdon, J. Mater. Sci. **44**, 5998 (2009).
3. O. A. Kaibyshev, Superplasticity of Alloys Intermetallides and Ceramics. Berlin: Springer-Verlag, (1992).
4. G. D. Bengough. J. Inst. Metals **7**, 123 (1912).
5. S. H. Xia, J. Wang, J. T. Wang, J. Q. Liu, Mater. Sci. Eng. A **493**, 111 (2008).
6. R. C. Cook, Superplasticity in a dilute zinc aluminum alloy, Master's Thesis, University of British Columbia, Canada, (1968).
7. T. K. Ha, J. R. Son, W. B. Lee, C. G. Park, Y. W. Chang, Mater. Sci. Eng. A **307**, 98 (2001).
8. H. Naziri, Superplasticity in Zn-based Alloys, Ph. D. Thesis, Cranfield Institute of Technology, United Kingdom, (1972).
9. P. *Málek P*., *Lukáč*, Czech. J. Phys. B **36**, 498 (1986).
10. T. Tanaka, K. Makii, A. Kushibe, M. Kohzu, K. Higashi, Scr. Mater. **49**, 361 (2003).
11. M. Demirtas, G. Purcek, H. Yanar, Z. J. Zhang, Z. F. Zhang, J. Alloys Compnd. **623**, 213 (2015).
12. T. Hirata, T. Tanaka, S. W. Chung, Y. Takigawa, K. Higashi, Scr. Mater. **56**, 477 (2007).
13. T. Tanaka, H. Watanabe, K. Higashi, Mater. Trans. **44**, 1891 (2003).
14. T. Tanaka, K. Higashi, Mater. Trans. **45**, 1261 (2004).
15. P. Kumar, C. Xu, T. G. Langdon, Mater. Sci. Eng. A **429**, 324 (2006).
16. Y. Huang, T. G. Langdon, J. Mater. Sci. **37**, 4993 (2002).
17. C. F. Yang, J. H. Pan, M. C. Chuang, J. Mater. Sci. **43**, 6260 (2008).
18. M. Demirtas, G. Purcek, H. Yanar, Z. J. Zhang, Z. F. Zhang, Mater. Sci. Eng. A **620**, 233 (2014).
19. K. Itatani, K. Tsuchiya, Y. Sakka, I. J. Davies, S. Koda, J. Eur. Ceram. Soc. **31**, 2641 (2011).
20. H. Yoshida, K. Matsui, Y. Ikuhara, J. Am. Ceram. Soc. **95**, 1701 (2012).
21. D. G. Garcia, S. B. Martin, B. M. Moshtaghioun, R. L. G. Romero, A. D. Rodriguez, Mater. Sci. Forum **735**, 120 (2013).
22. T. Ohkubo, T. Hiroshima, S. Ochiai, Y. Hirotsu, W. Fujitani, Y. Umakoshi, A. Inoue, Mater. Sci. Forum **304—306**, 361 (1999).
23. Y. Saotome, K. Itoh, T. Zhang, A. Inoue, Scr. Mater. **44**, 1541 (2001).
24. T. H. Alden, Trans. AIME **236**, 1633 (1966).
25. R. C. Gifkins, J. Inst. Met. **95**, 373 (1967).
26. M. M. I. Ahmed, T. G. Langdon, J. Mater. Sci. Letters **2**, 59 (1983).
27. Y. H. Zhu, Mater. Trans. **45**, 3083 (2004).
28. M. Kawasaki, T. G. Langdon, Mater. Sci. Eng. A **528**, 6140 (2011).
29. C. Y. Chou, S. L. Lee, J. C. Lin, C. M. Hsu, Scr. Mater. **57**, 972 (2007).
30. M. Kawasaki, T. G. Langdon, J. Mater. Sci. **42**, 1782 (2007).
31. P. Shariat, R. B. Vastava, T. G. Langdon, Acta Metall. **30**, 285 (1982).
32. P. Kumar, C. Xu, T. G. Langdon, Mater. Sci. Eng. A **410—411**, 447 (2005).
33. H. Naziri, R. Pearce, M. R. Brown, K. F. Hale, Acta Metall. **23**, 489 (1975).
34. I. I. Novikov, V. K. Portnoy, T. E. Terentieva, Acta Metall. **25**, 1139 (1977).
35. M. Kawasaki, T. G. Langdon, J. Mater. Sci. **48**, 4730 (2013).
36. T. S. Cho, H. J. Lee, B. Ahn, M. Kawasaki, T. G. Langdon, Acta Mater. **72**, 67 (2014).
37. B. P. Kashyap, A. K. Mukherjee, in: B. Baudelet, M. Suery (Eds.), Superplasticity, Paris: Centre National de la Recherché Scientifique (1985).